NTNU

TTT4205 Microwave Techniques

Waveguide assignment

Magne H. Å. Haneberg

November 11, 2015

1 Rectangular waveguide

1.1 Cut-off frequencies

The cut-off frequency of a hollow waveguide is given by

$$f_{\mathrm{c}}^{(\mathrm{mn})} = \frac{c}{2\pi\sqrt{\epsilon_{\mathrm{r}}\mu_{\mathrm{r}}}}\sqrt{\left(\frac{m\pi}{a}\right)^2 + \left(\frac{n\pi}{b}\right)^2}. \tag{1}$$

For a *WR75* waveguide, modes TE_{10} and TE_{20}, the cut-off frequencies are $f_{\mathrm{c}}^{(10)} = 7.8740\,\mathrm{GHz}$ and $f_{\mathrm{c}}^{(20)} = 15.748\,\mathrm{GHz}$.

The unimodal frequency band, ΔF, is given by

$$\Delta F = f_{\mathrm{c}}^{(20)} - f_{\mathrm{c}}^{(10)} = 7.8740\,\mathrm{GHz}. \tag{2}$$

1.2 Normalized propagation constants

The propagation constant of a hollow waveguide is given by

$$k_{\mathrm{z}}^{(\mathrm{mn})} = \sqrt{k_0^2\epsilon_{\mathrm{r}}\mu_{\mathrm{r}} - \left(\frac{m\pi}{a}\right)^2 - \left(\frac{n\pi}{b}\right)^2} \tag{3}$$

where

$$k_0 = \frac{2\pi f}{c} = \frac{2\pi f}{3\times 10^8\,\mathrm{m/s}}. \tag{4}$$

For a *WR75* waveguide, modes TE_{10} and TE_{20}, from 5 to 25 GHz, the propagation constants are shown in figure 1.

1.3 Phase and group velocities

The phase and group velocities for the TE_{10} mode in the unimodal frequency band is given by equations 5 and 6 and plotted in figure 2.

$$V_{\mathrm{ph}}^{(\mathrm{mn})} = \frac{\frac{c}{\sqrt{\epsilon_{\mathrm{r}}\mu_{\mathrm{r}}}}}{\sqrt{1-\left(\frac{f_{\mathrm{c}}^{(\mathrm{mn})}}{f}\right)^2}} \tag{5}$$

$$V_{\mathrm{g}}^{(\mathrm{mn})} = \frac{c}{\sqrt{\epsilon_{\mathrm{r}}\mu_{\mathrm{r}}}}\sqrt{1-\left(\frac{f_{\mathrm{c}}^{(\mathrm{mn})}}{f}\right)^2} \tag{6}$$

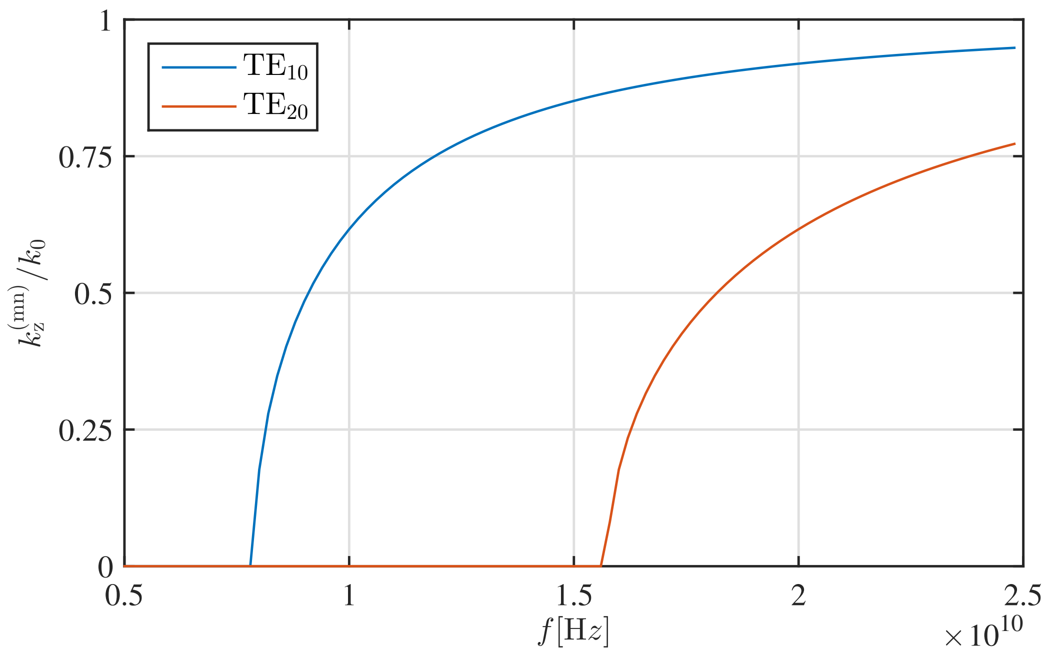

Figure 1: Normalized propagation constants in TE_{10} and TE_{20} modes.

1.4 Wave impedance

The wave impedance of a TE_{mn} mode is given by equation 7. This impedance is plotted for a TE_{10} wave in figure 3 for the unimodal frequency band.

$$W_{mn}^{TE} = \frac{\dot{E}_x^{(mn)}}{\dot{H}_y^{(mn)}} = \frac{\omega \mu_r \mu_0}{k_z^{(mn)}} = \sqrt{\frac{\mu_r \mu_0}{\epsilon_r \epsilon_0}} \frac{1}{\sqrt{1 - \left(\frac{f_c^{(mn)}}{f}\right)^2}} \tag{7}$$

1.5 Cut-off frequencies in an ideal dielectric

The cut-off frequencies for a waveguide is given by equation 1. If the waveguide is filled with air, this corresponds to $\epsilon_r = 1$. When filled with a perfect dielectric, ϵ_r changes value. However, it is still a real number.

The cut-off frequencies of a *WR75* waveguide filled with a perfect dielectric, $\epsilon_r = 2.44$, are shown in table 1.

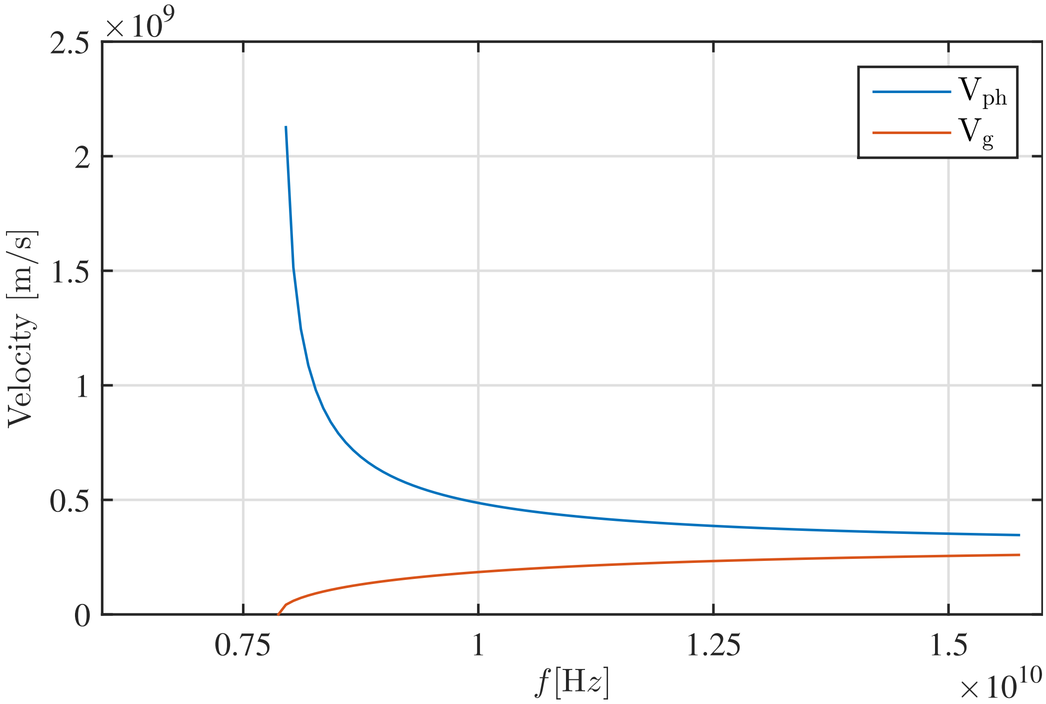

Figure 2: Phase and group velocities of TE_{10} wave in the unimodal frequency band

Table 1: Cut-off frequencies for waveguide filled with perfect dielectric

Mode	Cut-off frequency
TE_{10}	5.0408 GHz
TE_{20}	10.082 GHz

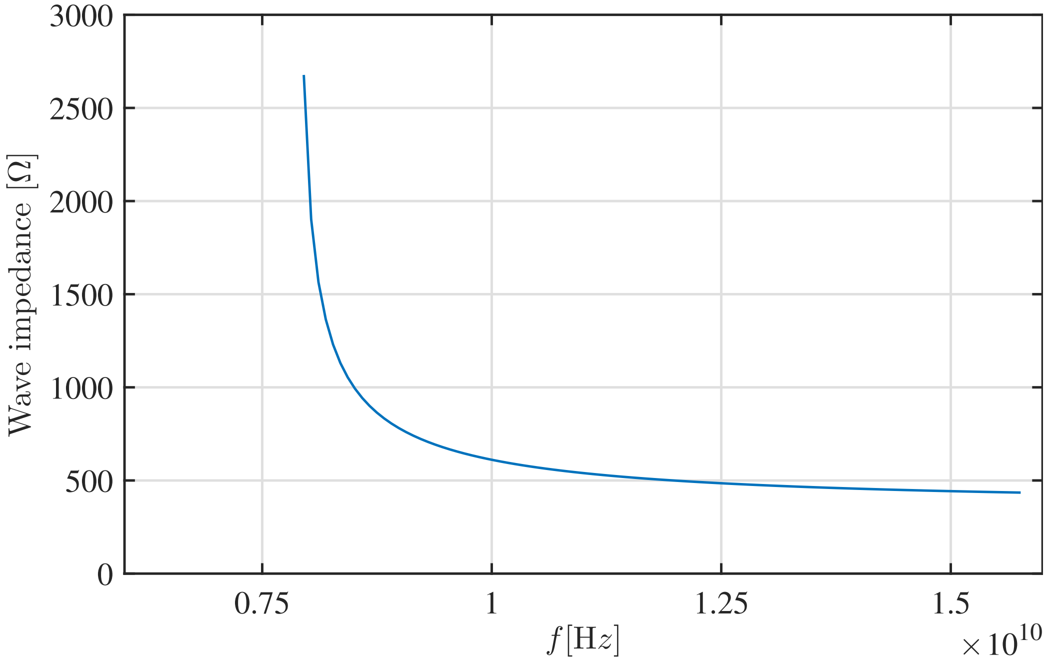

Figure 3: Wave impedance of TE_{10} wave in the unimodal frequency band

1.6 Dielectric loss constant

The dielectric loss constant for a mode TE_{mn} is given by equation 8.

$$\alpha_{\mathrm{d}}^{(\mathrm{mn})} = \frac{\Delta \bar{P}_{\mathrm{loss/unit}}}{2\bar{P}} \approx \frac{\epsilon_{\mathrm{r}}''}{\epsilon_{\mathrm{r}}'} \frac{\pi}{\lambda} \left(\frac{\Lambda_{\mathrm{mn}}}{\lambda} \right) \tag{8}$$

Λ_{mn} and λ are given by equations 9 and 10.

$$\Lambda_{\mathrm{mn}} = \frac{2\pi}{k_{\mathrm{z}}^{(\mathrm{mn})}} = \frac{\lambda}{\sqrt{1 - \left(\frac{f_{\mathrm{c}}^{(\mathrm{mn})}}{f} \right)^2}} \tag{9}$$

$$\lambda = \frac{2\pi}{k_0 \sqrt{\epsilon_{\mathrm{r}} \mu_{\mathrm{r}}}}. \tag{10}$$

According to [1],

$$\epsilon'' = \epsilon' \tan\delta = \epsilon_{\mathrm{r}} \epsilon_0 \tan\delta. \tag{11}$$

Given $\tan\delta = 0.002$, we have

$$\alpha_{\mathrm{d}}^{(\mathrm{mn})} \approx \frac{k_0 \sqrt{\epsilon_{\mathrm{r}} \mu_{\mathrm{r}}}}{1000 \sqrt{1 - \left(\frac{f_{\mathrm{c}}^{(\mathrm{mn})}}{f} \right)^2}}. \tag{12}$$

The dielectric loss constant is plotted for the unimodal frequency band in figure 4.

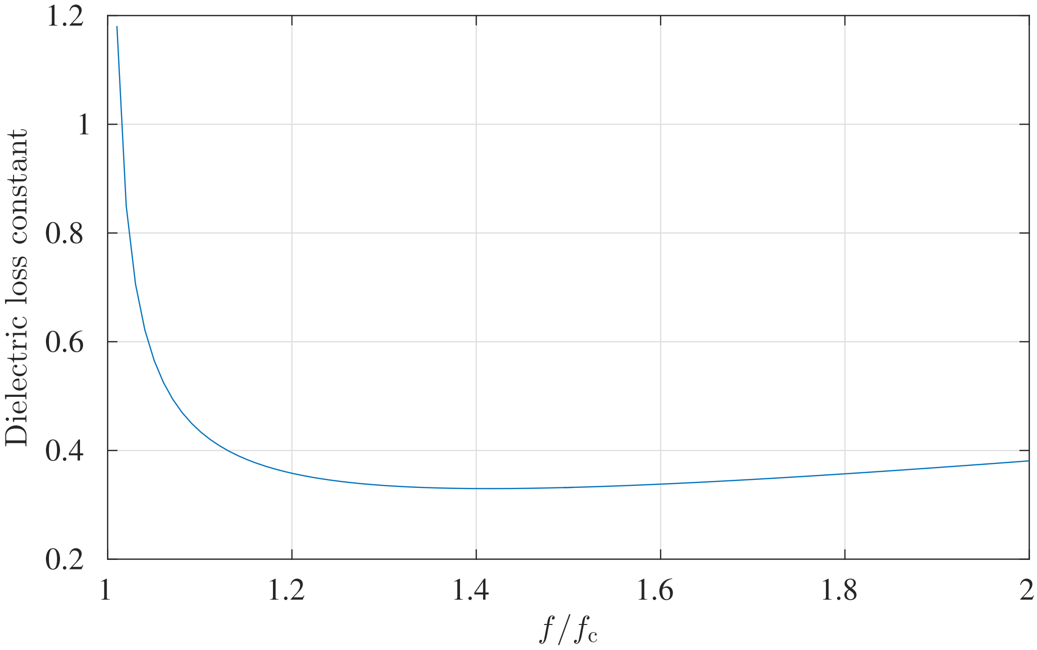

Figure 4: Dielectric loss constant, TE_{10} wave.

1.7 Equivalent capacitance and inductance

The equivalent capacitance and equivalent inductance are given by equations 13 and 14, respectively.

$$C_{\mathrm{equ}} \approx \frac{2k_{\mathrm{z}}^{(10)}b}{\pi^2 f W_{10}^{\mathrm{TE}}} \ln\left[\csc\left(\frac{\pi s}{2a}\right)\right] \tag{13}$$

$$L_{\mathrm{equ}} \approx \frac{a\mu_{\mathrm{r}}\mu_0}{2\pi\cot^2\left(\frac{\pi s}{2a}\left[1+\csc^2\left(\frac{\pi s}{2a}\right)\right]\right)} \tag{14}$$

The equivalent capacitance is plotted in figure 5.

The equivalent inductance does not vary with frequency. For the specified waveguide, $L_{\mathrm{equ}} \approx 2.1633 \times 10^{-8}$ H/m.

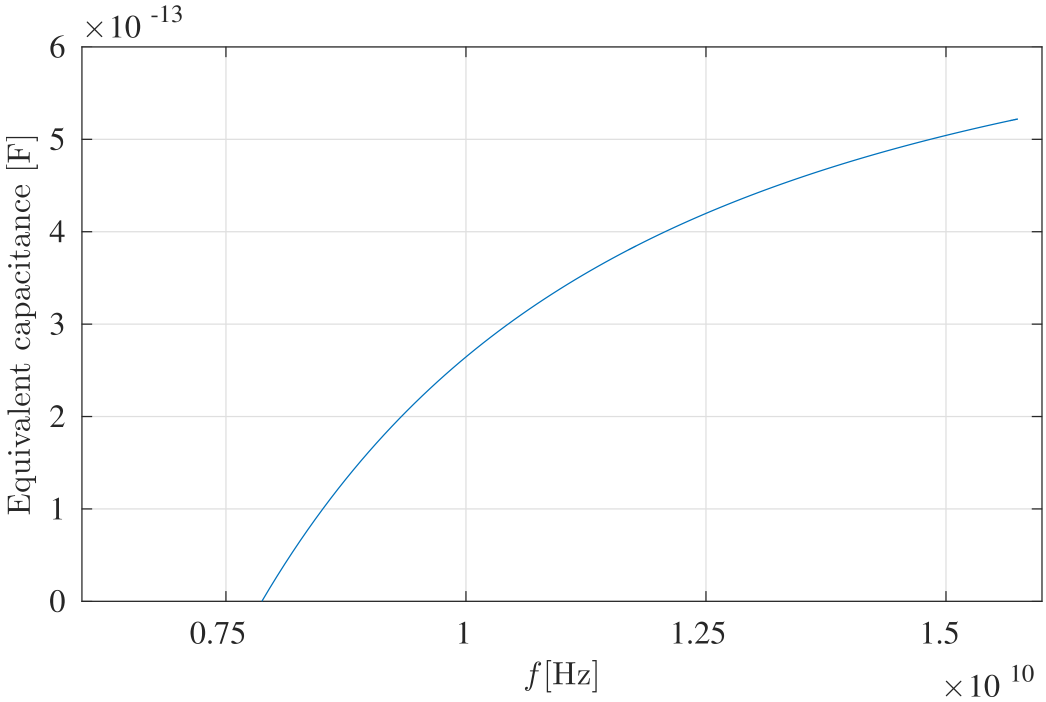

Figure 5: Equivalent capacitance over the unimodal frequency band.

2 Microstrip line

2.1 Effective permittivity

The effective permittivity relies on the geometry of the microstrip line. It is given by equation 15.

$$\epsilon_{\text{eff}}(f=0) = \left(\frac{\beta}{k_0}\right)^2 = \frac{\epsilon_{\text{r}}+1}{2} + \frac{\epsilon_{\text{r}}-1}{2\sqrt{1+\frac{10h}{W}}} \tag{15}$$

Given the geometry $h = 1\,\text{mm}$ and $W = (0.1\ldots4)\,\text{mm}$, with $\epsilon_{\text{r}} = 3.32$, the effective permittivity becomes as plotted in figure 6.

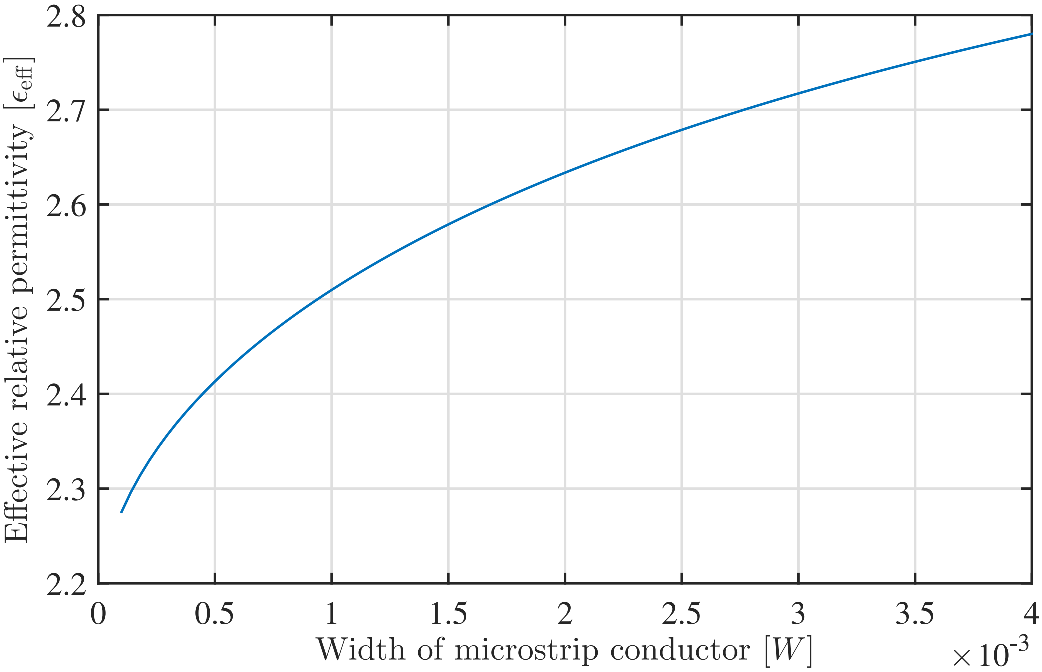

Figure 6: Effective relative permittivity of microstrip line.

2.2 Characteristic impedance

The characteristic impedance of a microstrip line is given by equation 16.

$$Z_c = \begin{cases} \frac{60}{\epsilon_{\text{eff}}(f=0)} \ln\left(\frac{8h}{W} + \frac{0.25W}{h}\right) & \frac{W}{h} < 1 \\ \frac{120\pi}{\sqrt{\epsilon_{\text{eff}}(f=0)}\left[\frac{W}{h}+1.393+0.667\ln\left(\frac{W}{h}+1.444\right)\right]} & \frac{W}{h} \geq 1 \end{cases} \tag{16}$$

Given the geometry $h = 1\,\text{mm}$ and $W = (0.1 \ldots 4)\,\text{mm}$, with $\epsilon_r = 3.32$, the characteristic impedance becomes as plotted in figure 7.

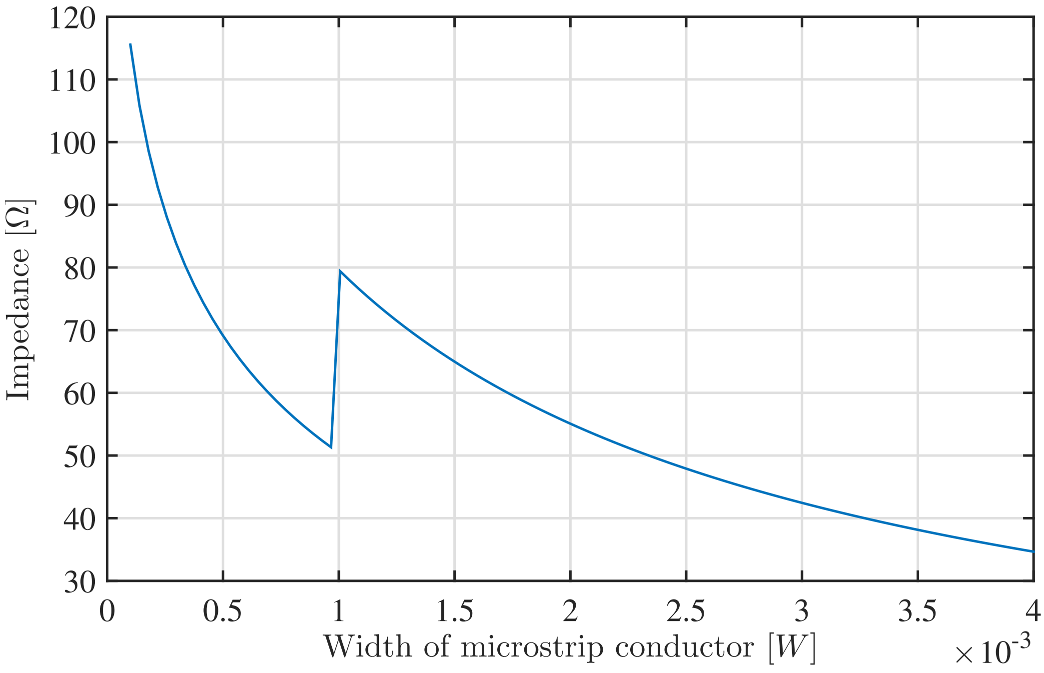

Figure 7: Characteristic impedance of microstrip line.

2.3 S-matrix coefficients

The S-matrix coefficients, transmission and reflection, are given by equations 17 and 18. They are plotted in figure 8.

$$T = \frac{2\sqrt{Z_c^{(2)} Z_c^{(1)}}}{Z_c^{(2)} + Z_c^{(1)}} \tag{17}$$

$$R = \frac{Z_c^{(2)} - Z_c^{(1)}}{Z_c^{(2)} + Z_c^{(1)}} \tag{18}$$

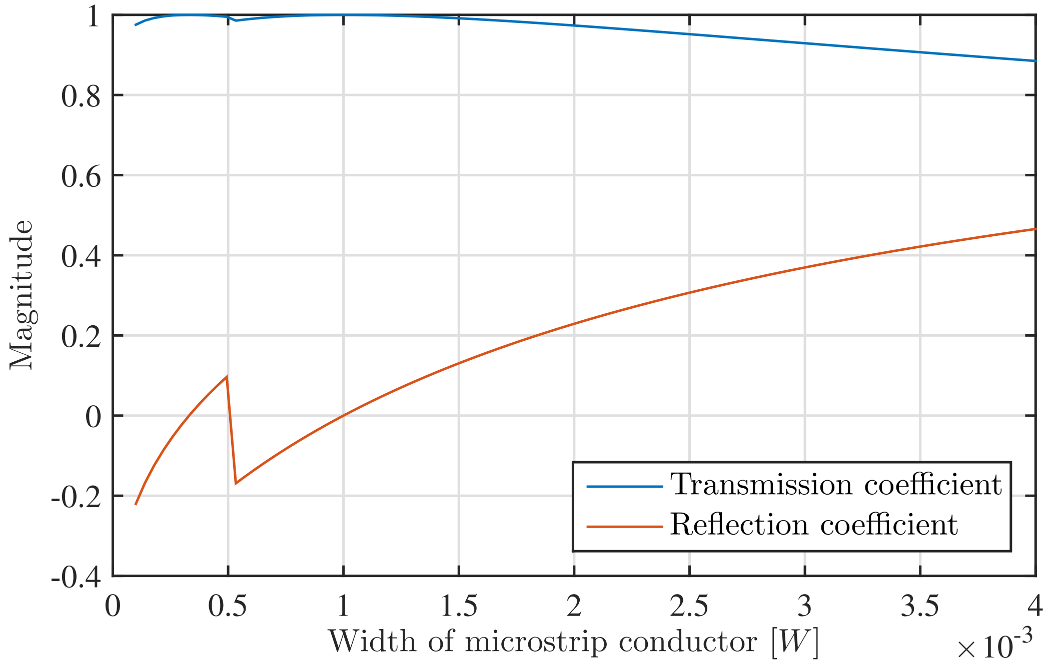

Figure 8: S-matrix coefficients of microstrip line.

3 Microstrip Branch-Line Directional Coupler

3.1 Calculating geometry of MS-BLDC

We want to design a Microstrip branch-line directional coupler with coupling and directivity ratios $-3\,\mathrm{dB}$ at the center frequency. The isolation ratio should be as low as possible.

The *Keysight ADS tools* can be used to calculate the geometry of a microstrip branch-line directional coupler. In order to use the ADS LineCalc utility, we have to obtain some parameters beforehand. These parameters are given by equations 19 and 20.

$$Z_{0,1} = Z_0\sqrt{1 - k_c^2} \tag{19}$$

$$Z_{0,2} = \frac{Z_{0,1}}{\sqrt{1 - \left(\frac{Z_{0,1}}{Z_0}\right)^2}} \tag{20}$$

Here k_c is given by

$$k_\mathrm{c} = \sqrt{\frac{P_\mathrm{c}}{P_\mathrm{i}}} = \sqrt{\frac{1}{2}} \tag{21}$$

where P_i is the incident power and P_c is the power in the coupled port. We also have to take into account that port 1, port 2 and port 4 are all a quarter wavelength away from each other. Therefore, ideally, the power on port 2 and 4 should be 90° out of phase. We shall examine this closer later.

Inserting the values in table 2 into ADS LineCalc, the results in table 3 are obtained.

Table 2: ADS LineCalc input parameters

Parameter	Size
F_0	1.6 GHz
h	1 mm
ϵ_r	3.32
Z_0	50 Ω
$Z_{0,1}$	35.3553 Ω
$Z_{0,2}$	50.0000 Ω
$\Delta\phi$	90°

Table 3: Branch-line coupler geometry

Parameter	Size
L50	28.8218 mm
W50	2.337 17 mm
L1	28.2112 mm
W1	3.910 89 mm
L2	28.8170 mm
W2	2.346 83 mm

3.2 Simulation of MS-BLDC

Figure 9 shows a model of the MS-BLDC in ADS.

Figure 10 shows a simulation of S(2,1) and S(4,1) in ADS. The markers indicate the peak values. We see that the components are in fact not exactly

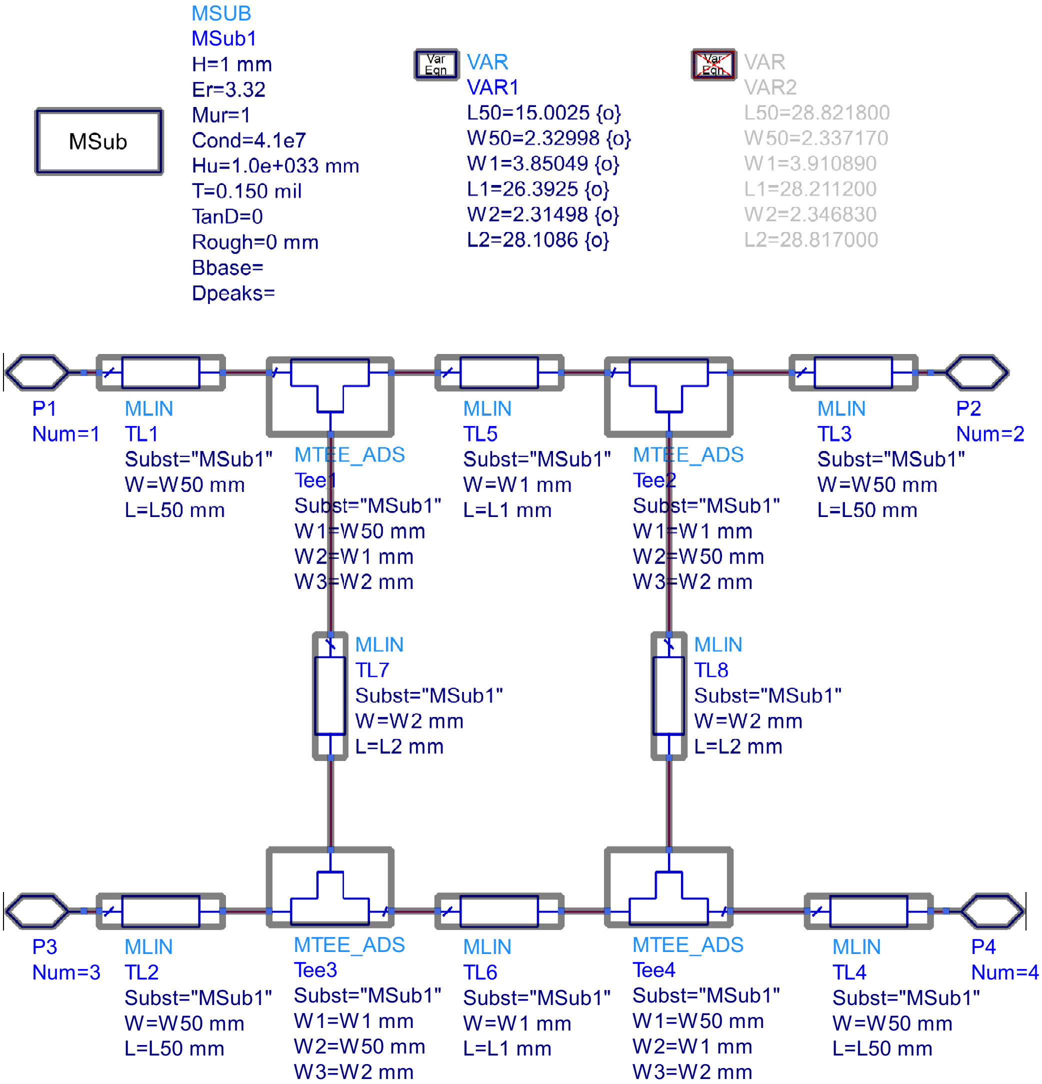

Figure 9: Model of Microstrip branch-line directional coupler in ADS.

−3 dB at 1.6 GHz. As can be seen from figure 11, the two components are approximately 90° out of phase.

3.3 In-depth electromagnetic simulation

To get an idea of how the design will behave in real life, a more thorough simulation is necessary. Figure 12 shows the test setup in *ADS Momentum*.

Running this simulation with optimization, we obtain a new geometry for the MS-BLDC. These values are exempt from this paper, but we note that they were very similar yet different from the initial values.

Figures 14 and 15 shows how this new, optimized geometry affects S(2,1) and S(4,1). Figure 13 shows the intensity of current in the MS-BLDC.

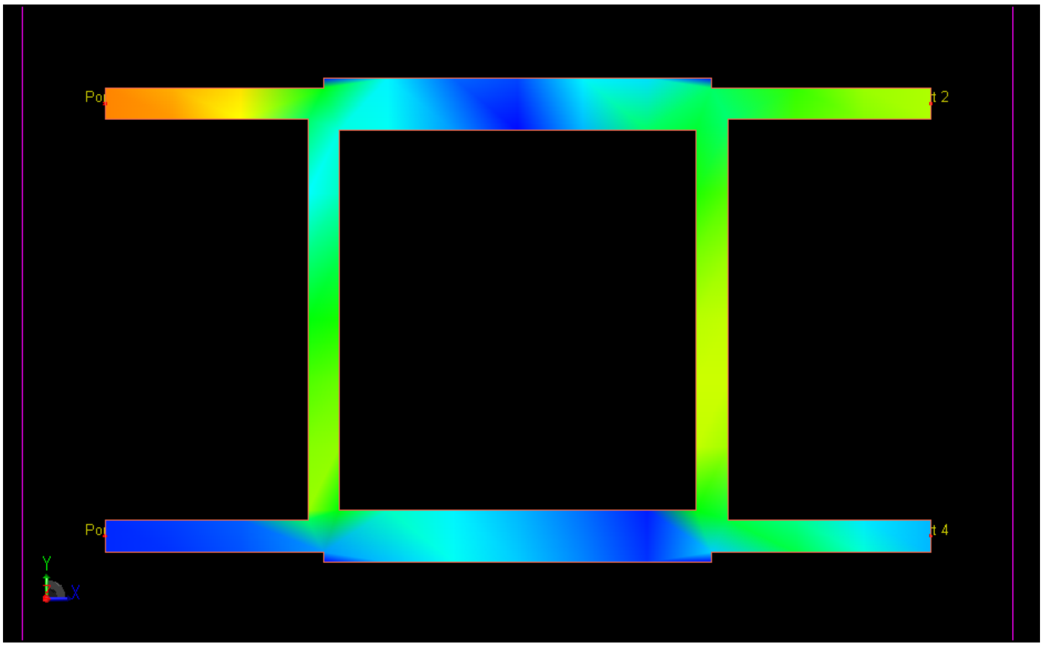

Figure 13: Simulated current intensity in MS-BLDC.

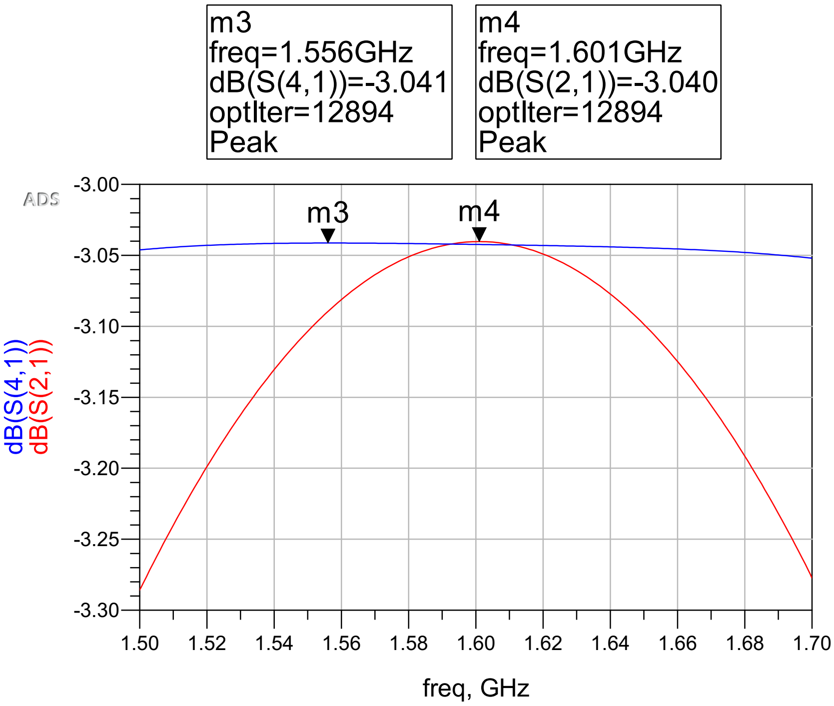

Figure 10: Simulated S-matrix components S(2,1) and S(4,1).

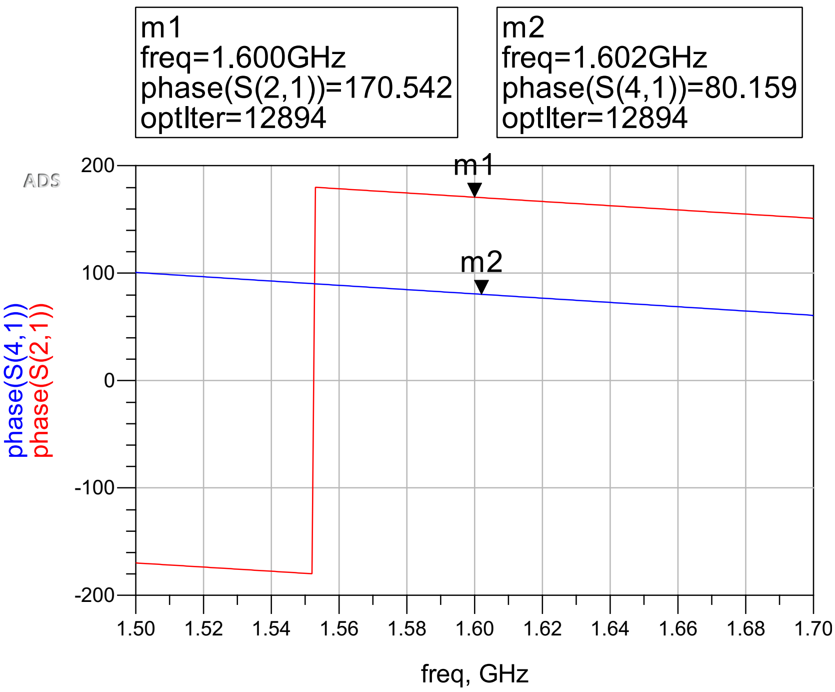

Figure 11: Simulated S(2,1) and S(4,1) phase difference.

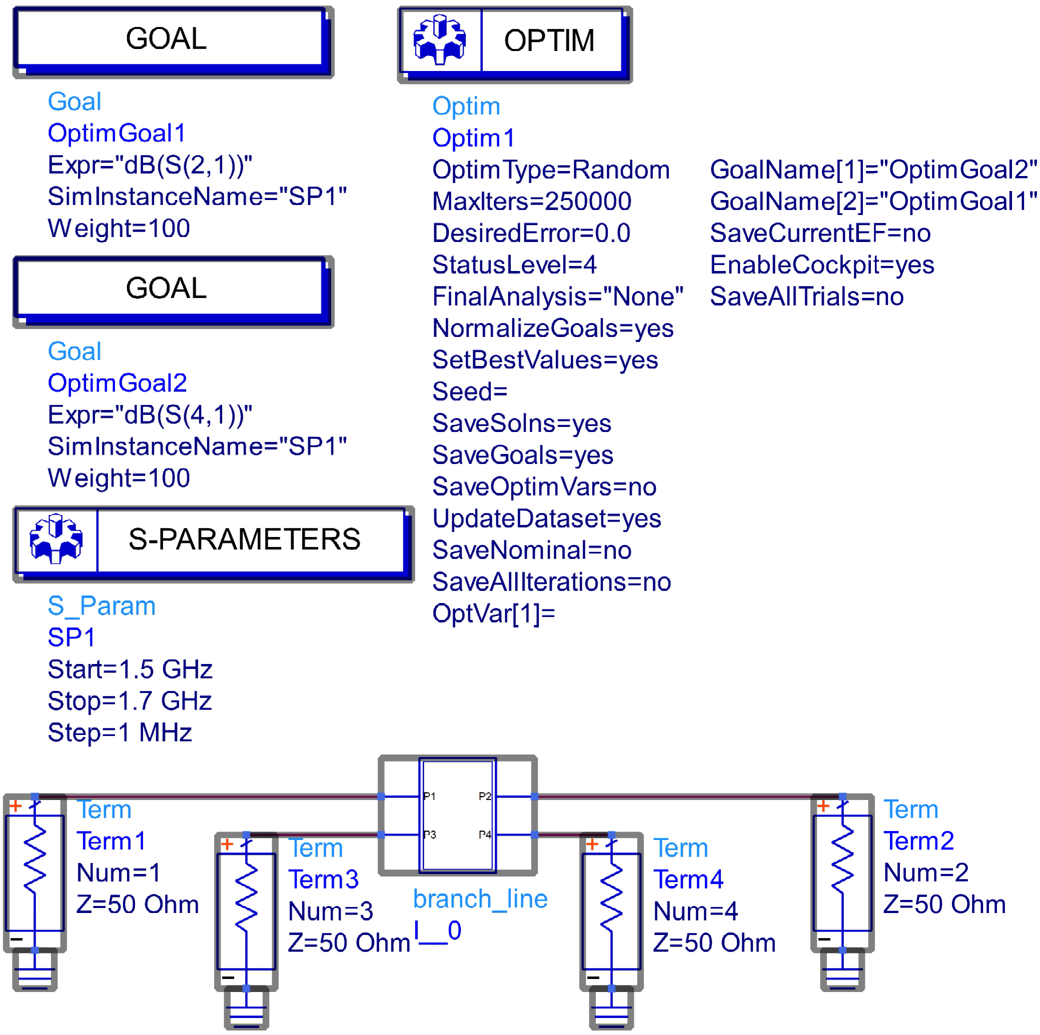

Figure 12: Simulation schematic in ADS.

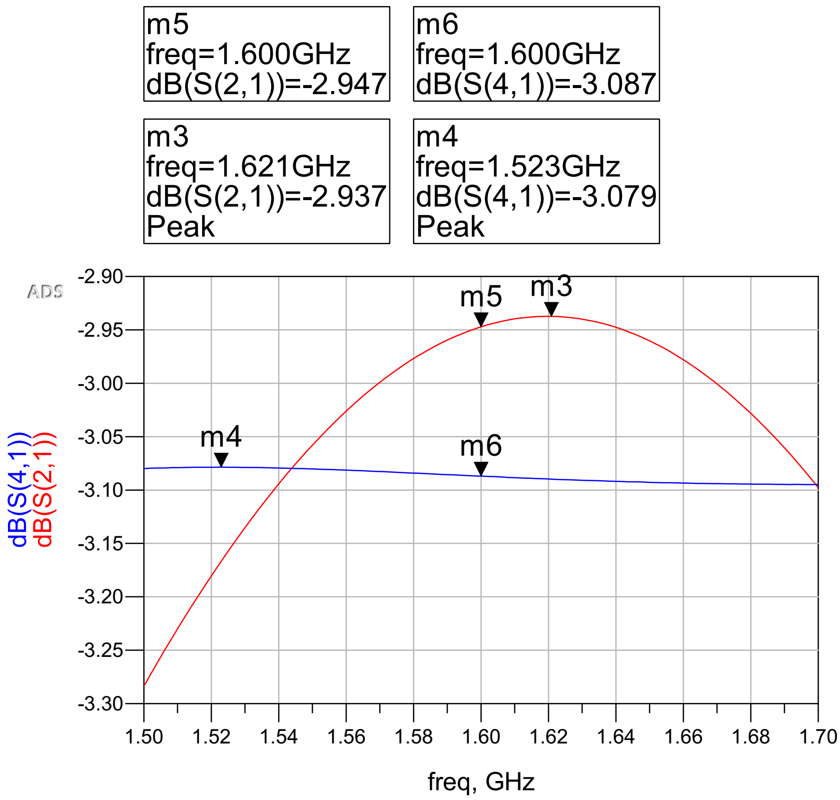

Figure 14: Simulated S(2,1) and S(4,1) with new geometry.

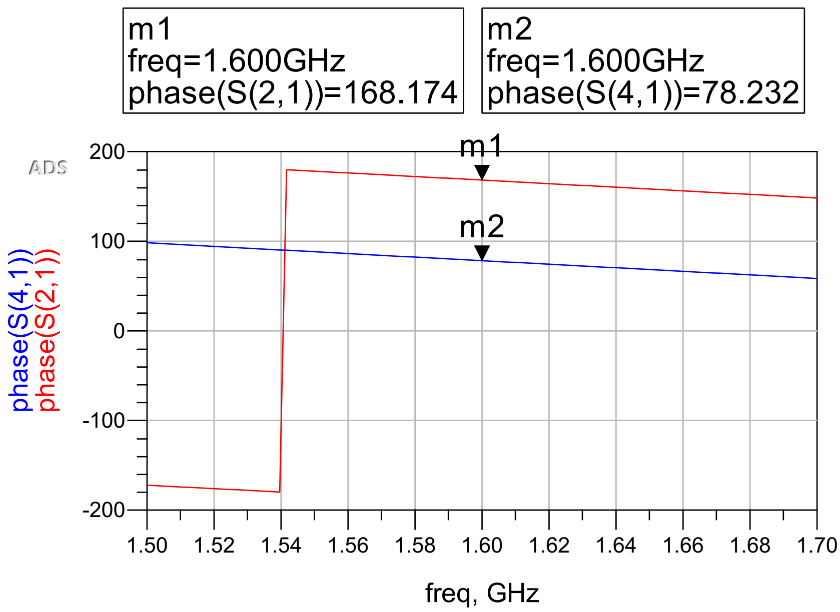

Figure 15: Simulated S(2,1) and S(4,1) phase difference with new geometry.

References

[1] David M. Pozar:
Microwave Engineering
Wiley & Sons,Inc., Fourth ed.